Behaviour of lithium and its isotopes during weathering in the Mackenzie Basin, Canada

Romain Millot, Nathalie Vigier, Jérôme Gaillardet

Behaviour of lithium and its isotopes during weathering in the Mackenzie Basin, Canada

Romain Millot (1)*, Nathalie Vigier (2) and Jérôme Gaillardet (3)

(1) BRGM, Metrology Monitoring Analysis Department, Orléans, France
* Corresponding author, e-mail: r.millot@brgm.fr

(2) CRPG, CNRS, Nancy-Université, Vandœuvre-lès-Nancy, France

(3) IPGP, Equipe de Géochimie et Cosmochimie, Université Paris 7, Paris, France

Abstract

We report Li isotopic compositions, for river waters and suspended sediments, of about 40 rivers sampled within the Mackenzie River Basin in northwestern Canada. The aim of this study is to characterize the behaviour of Li and its isotopes during weathering at the scale of a large mixed lithology basin. The Mackenzie river waters display systematically heavier Li isotopic compositions relative to source rocks and suspended sediments. The range in δ^7Li is larger in dissolved load (from +9.3 to +29.0‰) compared to suspended sediments (from -1.7 to +3.2‰), which are not significantly different from δ^7Li values in bedrocks. Our study shows that dissolved Li is essentially derived from the weathering of silicates and that its isotopic composition in the dissolved load is inversely correlated with its relative mobility when compared to Na. The highest enrichment of ^{7}Li in the dissolved load is reported when Li is not or poorly incorporated in secondary phases after its release into solution by mineral dissolution. This counterintuitive observation is interpreted by the mixing of water types derived from two different weathering regimes producing different Li isotopic compositions within the Mackenzie River Basin. The incipient weathering regime characterizing the Rocky Mountains and the Shield areas produces ^{7}Li enrichment in the fluid phase that is most simply explained by the precipitation of oxy-hydroxide phases fractionating Li isotopes. The second weathering regime is found in the lowland area and produces the lower δ^7Li waters (but still enriched in ^{7}Li compared to bedrocks) and the most Li-depleted waters (compared to Na). Fractionation factors suggest that the incorporation of Li in clay minerals is the mechanism that explains the isotopic composition of the lowland rivers. The correlation of boron and lithium concentrations found in the dissolved load of the Mackenzie rivers suggests that precipitation of clay minerals is favoured by the relatively high residence time of water in groundwater. In the Shield and Rocky mountains, Li isotopes suggest that clay minerals are not forming and that secondary minerals with stronger affinity for ^{7}Li appear.

Although the weathering mechanisms operating in the Mackenzie Basin need to be characterized more precisely, the Li isotope data reported here clearly show the control of Li isotopes by the weathering intensity. The spatial diversity of weathering regimes, resulting from a complex combination of factors such as topography, geology, climate and hydrology explains, in fine, the spatial distribution of Li isotopic ratios in the large drainage basin of the Mackenzie River. There is no simple relationship between Li isotopic composition and chemical denudation fluxes in the Mackenzie River Basin.

Keywords: lithium isotopes, river waters, silicate weathering, sediments, erosion, Mackenzie Basin

Submitted on September 22nd 2009 – Revised on April 22nd 2010

7 198 words (without the references and captions)

1. INTRODUCTION

Assessing the behaviour of lithium and the distribution of Li isotopes during weathering is of major importance for studying water/rock interactions at the surface of the Earth. This is because lithium (^{6}Li ~7.5% and ^{7}Li ~92.5%) is a fluid-mobile element and, due to the large relative mass difference between its two stable isotopes, it is subject to significant low temperature mass fractionation which provides key information on the nature of weathering processes.

Recent studies have shown that the range of δ^{7}Li values spans more than 40‰ at the Earth surface ($\delta^{7}Li = (^{7}Li/^{6}Li_{sample} / ^{7}Li/^{6}Li_{L\text{-}SVEC} -1) \times 10^{3}$), (e.g. Pistiner and Henderson 2003, Rudnick et al. 2004, Kisakürek et al. 2004, Huh et al. 2004, Kisakürek et al. 2005, Hathorne and James 2006, Pogge von Strandmann et al. 2006, Vigier et al. 2009). Furthermore, the world-wide range of δ^{7}Li in river waters is between +6 and +33‰ (Huh et al. 1998, 2001). There are as yet few studies concerning mixed lithology basins, but these suggest that river water δ^{7}Li is not affected by differences in catchment lithology (Kisakürek et al. 2005, Huh et al. 1998). Rather, lithium isotopes are thought to be strongly affected by isotope fractionation during secondary mineral formation and the degree and type of silicate weathering (Kisakürek et al. 2004, Huh et al. 2004, Kisakürek et al. 2005, Hathorne and James 2006, Pogge von Strandmann et al. 2006, Vigier et al. 2009).

To date, both the magnitude of the Li isotopic fractionation associated with water-rock interaction processes, and the factors controlling these fractionations, are poorly understood. However, both field and experimental studies have shown that ^{6}Li is preferentially retained by secondary minerals during silicate weathering (Pistiner and Henderson 2003, Kisakürek et al. 2004, Pogge von Strandmann et al. 2006, Vigier et al. 2009). Accordingly, the fractionation of Li isotopes is dependent upon the extent of chemical weathering. Large fractionation seems to occur during superficial weathering while little fractionation is observed during more

intense or prolonged weathering in stable environments (Huh et al. 1998, 2001, Pogge von Strandmann et al. 2006).

Lithium isotopic fractionation has been documented in numerous natural environments, with experimental and natural data (Huh et al. 2001, Pistiner and Henderson 2003, Tomascak 2004). It has been shown that partial dissolution of basalts does not result in fractionation of lithium isotopes, but that dissolution of granitic rock can cause fractionation (Pistiner and Henderson 2003). In addition, adsorption onto mineral surfaces can also be a mechanism of Li isotopic fractionation in the hydrosphere. Sorption of Li from aqueous solutions by mineral phases at the temperature of the Earth's surface has been highlighted by Taylor and Urey (1938), as well as by Anderson et al. (1989). Li sorption experiments utilizing several minerals (Pistiner and Henderson 2003) have revealed that Li isotopic fractionation does not occur when this element is not incorporated into the structure of the solid (physical sorption). When Li is incorporated by stronger bonds (chemical sorption), an isotopic fractionation is observed that is dependent on the chemical structure of the minerals (Anghel et al. 2002). The most significant Li isotopic fractionation factor ($\Delta_{\text{solution - solid}}$) ~ +14‰ has been measured for gibbsite. For Li sorption processes between solution and different solids (clay minerals such as kaolinite and vermiculite, and freshwater sediments), Zhang et al. (1998) have observed even higher Li isotopic fractionation factors ($\Delta_{\text{solution - solid}}$ ~ +22‰).

In the present paper, we have undertaken a systematic study of the weathering products (both dissolved load and suspended sediments) of the Mackenzie River Basin, one of the major high latitude river basins of North America. This area is of particular interest because it has previously been extensively studied and is well characterized from a lithology and weathering mass budget point of view (Vigier et al. 2001, Millot et al. 2002, Millot et al. 2003, Gaillardet et al. 2003). Also, there is a clear contrast between mountains and plains, with a fourfold increase of silicate chemical weathering rates in the plains (Millot et al. 2003). A direct comparison of silicate weathering rates and river Li isotope compositions can be performed. In this paper, we evaluate the potential of Li isotopes as a tracer of silicate weathering processes in large mixed lithology basins at the scale of a large river basin.

2. GEOLOGICAL SETTING AND SAMPLE LOCATIONS

This study focuses on the Mackenzie River basin and adjacent river basins (Stikine, Nass, Skeena, Fraser, and Yukon rivers). Most of the river waters and sediments are from the Mackenzie River Basin itself (Figure 1), which is located in northwestern Canada under arctic and subarctic climate. The mainstream of the Mackenzie River was sampled at two locations (samples CAN96-6 at the river mouth and CAN96-25 upstream). The main tributaries of the Mackenzie River are the Red Arctic River (CAN96-7), the Liard River (CAN96-26), the Peel River (CAN96-5), the Peace River (CAN96-15 and CAN96-37), the Slave River (CAN96-38) and the Athabasca River (CAN96-42).

The Mackenzie River basin is composed of three main structural units, corresponding to different geomorphological zones: namely, the Rocky and the Mackenzie Mountains in the western part, the Interior Platform (lowlands), and the Canadian Shield (in the eastern part), (Figure 1). Rivers belonging to a transition-zone correspond to basins draining the foothills located between the Rockies and the low-lying plains. From a mass budget point of view, the mainstream of the Mackenzie is mostly fed by tributaries draining the Interior Plain. River samples from the adjacent basins of the Yukon and Fraser Rivers are also considered here because their geological contexts are similar to those of the Upper Liard and Athabasca sub-basins, both located in the Rocky Mountains. Finally, the main rivers draining the Western Canadian orogenic belt were also analysed (Nass, Skeena and Stikine River).

Sampled rivers therefore drain a large range of lithologies: volcanics and immature volcano-clastic sediments in the Western Canadian orogenic belt (Stikine terrane), carbonates and slates in the Mackenzie Mountains, marine and non-marine sedimentary rocks (Cambrian to Cretaceous limestones, shales and sandstones) in the Interior plains of the basin, and old silicate rocks (Archean granites and gneisses) in the Slave Province of the Canadian Shield.

The chemical weathering conditions and physical erosion rates differ greatly depending on the runoff and basin lithology. Chemical denudation rates in this arctic zone are rather low

compared to other major river basins, as determined by Millot et al. (2003) and Gaillardet et al. (2003). Full details concerning river samples (geological and hydrological contexts) have been published in Millot et al. (2003) for the Mackenzie River basin, in Millot et al. (2002) for the rivers of the Canadian Shield and in Gaillardet et al. (2003) for rivers of the Western Cordillera.

3. ANALYTICAL METHODS

3.1. Sampling methodology, major and trace element concentration measurements

River waters were sampled twice during the high flow stage of the summer season (August 1996 and June 1999). In the field, 10-15 L of river water was collected in acid-washed containers for major and trace elements, and isotopic measurements (Millot et al. 2003). Samples were filtered a few hours later, using a Sartorius frontal filtration unit (0.2 µm cellulose acetate filter, 142 mm diameter). After filtration, samples were stored in acid-washed polypropylene bottles. The river sediments were collected after drying and centrifugation of the retentate of river water filtration. The samples for cations and trace element concentrations and Li isotope analyses were acidified to pH = 2 with ultrapure HNO_3. Bottles for anion analyses were not acidified.

Lithium concentrations (for river waters and suspended sediment samples) were determined by ICP-MS (VG PlasmaQuad II+) with indium as an internal standard, with a precision of ± 5%.

Major and trace elements are reported in Millot et al. (2003) for the Mackenzie River basin, in Millot et al. (2002) for the rivers of the Canadian Shield, and in Gaillardet et al. (2003) for rivers of the Western Cordillera respectively.

3.2. Lithium isotope measurements

Lithium isotopic compositions were measured using a Neptune Multi-Collector ICP-MS (Millot et al. 2004). $^{7}Li/^{6}Li$ ratios were normalized to the L-SVEC standard solution (NIST SRM 8545, Flesch et al. 1973) following the standard-sample bracketing method. Typical in-run precision on the determination of $\delta^{7}Li$ is about 0.1-0.2‰ ($2\sigma_m$, standard error of the mean).

Chemical separation of Li from the matrix was achieved before isotope analyses, following a procedure modified from the technique of James and Palmer (2000) that uses a cationic exchange resin (a single column filled with 3 mL of BioRad AG® 50W-X12 resin, 200-400 mesh) and HCl acid media (0.2N) for 30 ng of Li. Blanks for the total chemical extraction were less than 30 pg of Li, which is negligible since this represents a blank/sample ratio of $<10^{-3}$.

Successful quantitative measurement of Li isotopic compositions requires 100% Li recovery during laboratory processing. Therefore, frequent column calibrations were performed and repeated analysis of L-SVEC standard processed through the columns shows that no isotope fractionation occurred as a result of the purification process.

Accuracy and reproducibility of the isotopic measurements were tested by repeated analyses of three Li standard solutions (namely ^{6}Li-N, LiCl-N and ^{7}Li-N, Carignan et al. 2007). Mean values of $\delta^{7}Li$ = -8.0‰ $\pm$ 0.3 (2σ, n = 38), $\delta^{7}Li$ = +10.1‰ $\pm$ 0.2 (2σ, n = 46) and $\delta^{7}Li$ = +30.2‰ $\pm$ 0.3 (2σ, n = 89), were obtained for ^{6}Li-N, LiCl-N and ^{7}Li-N respectively over a period of 10 months. Thus, long-term reproducibility of the Li mass analysis is better than 0.3‰ at the two sigma level for standard solutions (σ: standard deviation).

The accuracy and reproducibility of the entire method (purification procedure + mass analysis) were tested by repeated measurement of a seawater standard solution (IRMM BCR-403) after separation of Li from the matrix, for which we obtained a mean value of $\delta^{7}Li$ = +30.8‰ $\pm$ 0.4 (2σ, n = 15) over the period of the duration of the analyzes. This mean value is in a good agreement with our long-term measurements ($\delta^{7}Li$ = +31.0‰ $\pm$ 0.5, 2σ, n = 30, Millot et al. 2004) and with other values reported in the literature (see for example Carignan et al. 2004 and Tomascak 2004 for a compilation).

For suspended sediments, as well as for sands and rocks, a total digestion of 50 mg of crushed sample was performed over 4 days at 100°C in a closed beaker with a mixture of three ultrapure acids: 4 mL of HF (23N), 1 mL of HNO_3 (14N) and 0.1 mL of $HClO_4$ (12N). The solution was subsequently evaporated to dryness and 4 mL of HCl acid (6N) was added and left for a further 4 days at 100°C. Sample aliquots (30 ng of Li) of the residue of the acid dissolution were then dissolved in 0.5 mL of HCl (0.2N), before being placed on cation exchange columns for Li separation. Accuracy and reproducibility of the procedure for solid samples (dissolution + purification procedure + mass analysis) were tested by repeated measurement of the JB-2 basalt standard (Geological Survey of Japan) which gave a mean value of δ^7Li = +4.9‰ $\pm$ 0.6 (2σ, n = 17), in good agreement with published values (see Jeffcoate et al. 2004, Tomascak 2004 and Carignan et al. 2007 for data compilation).

4. RESULTS

4.1. Dissolved phase

Lithium concentrations (Table 1) in the Mackenzie basin river waters display a wide range of values, from 0.05 µmol/L (for the Skeena River in the W. Cordillera) to 1.29 µmol/L (for the Hay River located in the lowlands). The Mackenzie River at the river mouth (CAN96-6) has a Li concentration of 0.57 µmol/L. The main tributaries, which are mainly located in the low-lying plains, show a mean value of Li of 0.63 µmol/L, (n = 11). The group of rivers draining the Interior Platform display the highest Li contents (mean value of 0.85 µmol/L, n = 9). In contrast, rivers of the Shield and the W. Cordillera areas display the lowest Li levels (~0.16 µmol/L, n = 4 and ~0.08 µmol/L, n = 3, respectively). Also, rivers draining the Rocky Mountains have low Li contents (mean value of 0.30 µmol/L, n = 11). Finally, Li contents for rivers located in the transition zone are intermediate between those from the Rockies and those from the low-lying plains (mean Li = 0.54 µmol/L, n = 4).

Compared to the concentrations of dissolved Li reported in the pioneering work of Reeder et al. (1972) for the Mackenzie river system (Li ranging from <0.7 to 4.5 µmol/L), our values are clearly lower in the present case (from 0.05 to 1.29 µmol/L). This difference is likely to be related to the method used for the Li determination in waters. Indeed, Reeder et al. (1972) reported a detection limit of 0.70 µmol/L (~5 µg/L) by atomic adsorption in the early 1970's, whereas it is now ~0.01 µmol/L using modern ICP-MS techniques. Consequently, it is obvious that Reeder et al. (1972) were not able to measure low lithium concentrations in some of the rivers of the Mackenzie Basin (indeed Li was not detected in 49 samples of their suite of 101 river samples).

Lithium isotopic compositions in the Mackenzie river waters (Table 1) range from δ^7Li = +9.3 (for the Smoky River located in the transition zone) to +29.0‰ (for the Yellowknife River located in the Slave Province). Rivers from the Lowland regions vary from +10.1‰ to +16.8‰ with an average of +13.2‰. Rivers from the Rockies display higher δ^7Li values (from +12.2‰ to +20.5‰, with an average of +15.7‰), when compared to rivers draining the plains. Rivers draining the W. Cordillera and the Canadian Shield show the heaviest isotope compositions, with δ^7Li ranging between +25.2 to +29.0‰ for the Shield rivers and between +21.6 and +24.9‰ for the western orogenic belt (Stikine terrane).

An inverse relationship of Li isotopic composition with Li concentrations is observed for the Mackenzie river system (Figure 2). It is clear from this figure that the different physiographic provinces in the basin are characterized by different domains. The large tributaries display δ^7Li values that essentially reflect the mixture of waters from the mountains and waters from the lowlands, in the range +12.7 to +16.5‰ (with an average of +14.6‰). The Mackenzie River at river mouth (CAN96-6) shows a δ^7Li value of +15.0‰, close to both values reported by Huh et al. (1998) for the Mackenzie river mainstream (+17.9 and +15.7‰, respectively).

4.2. River sediments and bedrocks

Lithium concentrations in suspended sediments of the Mackenzie basin rivers (Table 2) range between 17.8 µg/g (for the Mackenzie River at river mouth) and 57.8 µg/g (for the Trout River in the Rockies). Lithium contents of the Mackenzie suspended sediments show almost the same range as that determined for the suspended sediments of the Orinoco basin (from 5.2 to 71.3 µg/g, see Huh et al. 2001) and are close to the mean value of 35 $\pm$ 11 µg/g reported for the Upper Continental Crust (UCC) by Teng et al. (2004).

The isotopic composition of the suspended sediments range from -1.7‰ to +3.2‰, with a mean value of +0.4‰ (n = 20, Table 2), identical, within uncertainties, to the estimate of the UCC (δ^7Li from -2 to +2 ‰, Teng et al. 2004). Suspended sediments from the main tributaries of the Mackenzie Basin display slightly negative δ^7Li values (from -1.6 to -0.2‰) whereas δ^7Li of suspended sediments of rivers located in the Rocky Mountains are slightly positive (from +0.3 to +3.2‰). The suspended sediments of the Nass and Stikine Rivers (W. Cordillera) exhibit positive and similar isotope signatures (δ^7Li = +1.0 and +1.2‰ respectively). As for Li content, the range of δ^7Li for suspended sediments of the Mackenzie Basin is comparable with the values obtained by Huh et al. (2001) for silicate regions of the Orinoco Basin. δ^7Li values measured in suspended sediments are also in good agreement with the range reported by Kisakürek et al. (2005) for the Himalayan rivers (-3.9 to +3.0‰).

The sand sample collected at the mouth of the Mackenzie River (CAN96-6) has a Li concentration of 47.4 µg/g, which is lower than the Li content of the corresponding suspended material (57.8 µg/g) and a Li isotopic composition of -0.5‰, not significantly different from that of the corresponding suspended sediments (-0.9‰).

Bedrocks (carbonates and black shales) sampled in the basin, and assumed to be representative of the main type of rocks exposures, display Li contents ranging between 1.5 and 64.4 µg/g (Table 3). The carbonate samples from the Rocky Mountains (CAN99-65) display the lowest concentration (1.5 µg/g), in agreement with literature data reported for other carbonates (e.g. Huh et al. 2001, Hathorne and James 2006). In contrast, Li contents in blackshales from the Interior Platform are high (29.1 and 64.4 µg/g). Two glacial tills sampled

within the Slave Province (Yellowknife and Prosperous Lake) display different Li concentrations of 16.2 and 54.6 µg/g respectively.

The carbonate sample (CAN99-65, Rocky Mountains) has the highest δ^7Li value (+7.2‰), in agreement with other values reported for continental carbonates by Huh et al. (2001). This value is likely to reflect a mixing between pure marine carbonate (δ^7Li > +25‰, Tomascak 2004, Hall et al. 2005, Hathorne and James 2006, Vigier et al. 2007) and detrital phases with much lower δ^7Li values and higher Li contents. δ^7Li for the blackshales are negative (-1.0 and -1.1‰ for the Interior plains and for the Transition zone samples respectively), but remain close to the estimate of the UCC. Finally, the two glacial till samples display relatively similar δ^7Li values of +4.8 and +5.2‰ respectively.

5. DISCUSSION

5.1. Sources of dissolved lithium

The sources of dissolved lithium in the river waters of the Mackenzie Basin can be assumed to be either released by rock weathering (including solubilisation of the bedrock, and destabilisation or desorption from secondary minerals), derived from the atmosphere (via precipitation or wet deposition), or derived from groundwater input. First of all, atmospheric input can be evaluated using chloride concentrations if no evaporite is present within the drainage basin. This is the case for most of the rivers of the Mackenzie Basin, as shown by Millot et al. (2002), Millot et al. (2003) and Gaillardet et al. (2003). In particular, rivers draining the Shield area, characterized by low chemical weathering rates, are good candidates for estimating the atmospheric input of Li. Rivers draining the Canadian Shield have low dissolved Li contents (from 0.07 to 0.2 µmol/L) and display the highest δ^7Li values, close to that of the ocean (δ^7Li = +31.0‰), a priori suggesting a marine origin for Li via seasalt input through precipitation. Then, if we assume that all chloride in the Shield rivers (with Li/Cl =

290 $5x10^{-3}$ and δ^7Li = +25.2‰ on average) is of atmospheric origin and that marine salts have
291 seawater Li/Cl molar ratios of $5x10^{-5}$ and δ^7Li = +31.0‰, it can be calculated that only a small
292 fraction of riverine Li (< 1%) in these rivers originates from seasalt input through precipitation.
293 The same calculation for rivers draining the Western Cordillera (i.e. the rainy region: 1500-
294 1750 mm/year compared to 350 mm/yr in the Shield area) indicates that a maximum of only
295 ~0.4% riverine Li could have been supplied by precipitation.
296 We provided evidence in a previous paper (Millot et al. 2002), that the rivers of the Shield
297 area (Slave Province) are characterized by a chloride excess compared to a pure marine
298 input, and we attributed their relatively high Cl concentrations to the dissolution of evaporite-
299 type aerosols derived from the dry area located south of the Great Slave Lake. Cambrian
300 evaporites occur at the base of the sedimentary basin of the lowlands, and these have
301 contributed to redeposited salt in modern lakes. The Salt River is one of the rivers that is
302 highly influenced by the dissolution of these formations. Although this river was not analysed
303 in the present work, Li and Na concentrations of the Salt River (Li = 4.5 µmol/L and Na =
304 276.45 mmol/L) have been reported by Reeder et al. (1972). The typical Li/Na ratio of this
305 river is $1.6x10^{-5}$ mol/mol. Considering this ratio along with the highest Cl concentration found
306 in rivers draining the Slave Province (80 µmol/L), we estimate there is a negligible Li input
307 from evaporites in the Shield rivers (less than 0.4% of lithium derived from evaporite).
308 In summary, our calculations indicate that the contribution of Li coming from precipitation and
309 wet deposition is negligible, and that dissolved Li in all sampled rivers is mainly derived from
310 weathering of silicate and carbonate rocks. Although carbonates have relatively low Li
311 concentrations (< 1 µg/g) compared to silicates (higher than 50 µg/g), their higher dissolution
312 rates may make them a significant source of Li in carbonate rich-regions. Millot et al. (2002)
313 showed that the areas of the Mackenzie Basin which are most influenced by carbonate
314 dissolution are the Rocky and Mackenzie Mountains. In contrast, the lowlands are less
315 influenced by this lithology and the Shield area displays no input from carbonate weathering.
316 The proportions of lithium derived from silicate and carbonate weathering can be calculated
317 from the results of the inversion model (Millot et al. 2003) which allowed us to determine, for

each major element present in the dissolved phase, the proportion derived from the weathering of silicate and carbonate end-members within the Mackenzie River Basin. We use a mean Li/Ca molar ratio of $15x10^{-6}$ for carbonates, in agreement with Li/Ca molar ratios ranging from $10x10^{-6}$ to about $20x10^{-6}$ reported in carbonates elsewhere (Hall and Chan 2004, Lear and Rosenthal 2006, Hathorne et al. 2009), and determine that the carbonate end-member contribution is very low for lithium. Between 90.5% and 99.4% of dissolved lithium is thus derived from silicate weathering in the Mackenzie River Basin (Figure 3).

These estimates agree well with previous studies that have inferred that most riverine Li derives from silicate lithologies (Huh et al. 1998, Kisakürek et al. 2005). In addition, the absence of a correlation between Li and Sr isotopic ratios (from Millot et al. 2003) argues against a carbonate weathering control on riverine Li isotopic composition. We therefore conclude that Li concentrations in the dissolved load of rivers in the Mackenzie Basin are essentially controlled by silicate weathering. Dissolved Li isotopic compositions are however highly variable within the Mackenzie river basin (from +9.3 to +29.0‰), suggesting variable fractionation of Li isotopes during silicate weathering.

5.2. Li isotopes and silicate weathering regimes

5.2.1. Evidence for isotope fractionation during chemical weathering

River dissolved loads are systematically enriched in ^{7}Li relative to bedrocks and suspended particles (Figure 4). In this regard, lithium is similar to boron (Lemarchand and Gaillardet 2006). However, the dissolved loads exhibit a large range of δ^{7}Li values across the sampled rivers. A part of this variability may derive from the δ^{7}Li of bedrocks, which might differ between the main provinces of the Mackenzie Basin. Literature data indicate that the Li isotopic composition of continental granites (-2 to +3‰, Teng et al. 2004, 2006, 2008, 2009) is slightly different from the shales and loesses from which they were derived (-3 to +5‰). The Li isotopic composition of the Canadian Shield bedrock (mainly consisting of granites

346 and associated crystalline rocks, Millot et al. 2002) is averaged in the glacial till samples
347 reported in Table 3. In concordance with literature data, the δ^7Li values measured in till
348 samples are higher than those measured in the bedrocks from the lowlands and the Rocky
349 Mountains (which are mainly recycled materials such as shales, blackshales, slates and a
350 few low grade metamorphic rocks). In Figure 4, we report δ^7Li values in silicate bedrocks
351 compiled from the literature together with the results from this study. Suspended sediment
352 and sand samples from the Mackenzie rivers fall within the range of bedrocks defined by our
353 bedrock samples and by literature data (Figure 4). However, a positive trend between δ^7Li
354 and Na/Al is observed (Figure 5). Due to the high solubility of Na during chemical weathering
355 compared to Al which is immobile, the Na/Al ratio can be regarded as “a weathering index”.
356 The low Na/Al ratios associated with low δ^7Li values suggests that lithium isotopes are
357 fractionated by chemical weathering processes. The direction of the fractionation in the
358 suspended sediments is consistent with the enrichment of ^{7}Li in the dissolved load since the
359 lowest Na/Al are associated with the lowest δ^7Li. Since the suspended sediments of the
360 Mackenzie rivers are essentially derived from sedimentary rocks (the Shield area does not
361 contribute significant sediment), it is difficult to conclude whether the Na loss recorded in the
362 Na/Al ratio is due to present day weathering conditions, or whether the low Na/Al ratios are
363 inherited from previous cycles of erosion and sedimentation. Examples of shale composites
364 reported in the literature, such as the PAAS or NASC (Post Archean Australian Shale and
365 North American Shale Composite: Holland 1978, Taylor and MacLennan 1985) do indeed
366 show Na depletion compared to granodioritic Upper Continental Crust (Taylor and
367 MacLennan 1985, Gaillardet et al. 1999). Given the low grade silicate weathering in the
368 Mackenzie River Basin (Millot et al. 2003), and the overlap of bedrock and suspended
369 sediment Li isotopes compositions (Figure 4), we favour the hypothesis that Na/Al in the
370 suspended sediments essentially records bedrock geochemistry rather than present day
371 weathering products. Therefore the trend of increasing Li isotopic composition with Na/Al
372 ratio (Figure 5) is likely inherited from the bedrock history. From a mass budget perspective,

it is not easy to estimate the partitioning of Li transported in the dissolved and particulate load because chemical weathering does not proceed at steady state (Vigier et al. 2001). However, the above considerations suggest that the dissolved load clearly reflects the fractionation of Li isotopes during chemical weathering (with the enrichment of ^{7}Li in the fluid), while the suspended phase is not significantly different from the bedrock. In other words, the dissolved load is sensitive to water rock interactions, but solids are not, because chemical weathering is too weak. Investigating in more detail the isotopic composition of Li in river suspended sediments as a function of weathering rate is beyond the scope of the present paper, but would be interesting to do at large scale. The next section focuses on the dissolved load.

5.2.2. Influence of the weathering regime

We show in the following that the range of Li isotopic composition measured in the rivers of the Mackenzie Basin is related to the weathering regime.

The Li/Na* ratio in the dissolved load, when compared to that in the bedrock can be used as an index of Li mobility compared to Na. Both elements are alkali metals, thus mobile during water-rock interactions. As shown by a number of previous studies, in contrast to Na, Li is likely to be incorporated into secondary minerals, such as clays. By analogy with the study of Georg et al. (2007) concerning the mobility of Si isotopes during chemical weathering in Iceland , we can define f_{Li}, the fraction of Li remaining in solution relative to Na, as:

$$f_{Li} = \frac{(Li/Na^*)_{dissolved}}{(Li/Na)_{bedrock}} \quad . \qquad (1)$$

where Na* is the Na concentration corrected for atmospheric input and for evaporite dissolution using the results of Millot et al. (2003). Correction for evaporite dissolution only significantly affects a few samples. A value of 1 for f_{Li} means that chemical weathering is

400 congruent. While dissolution is usually thought to be incongruent, precipitation of secondary
401 phases is the most probable process that will fractionate Li and Na, Li being known to have
402 affinity for clay minerals, while Na is much more mobile and hardly reincorporated into clay
403 minerals.
404 We used the suspended sediment compositions, where available, to estimate the bedrock
405 Li/Na ratio. In the Canadian Shield province, because rivers at the time of sampling
406 contained very low levels of suspended sediment, we used two glacial till samples (Table 3)
407 which display contrasting Li/Na ratios. The calculated f_{Li} in the rivers of the Mackenzie basin
408 range between 0.1 (in the lowlands and main tributaries) to 0.8 in the rivers of the Shield
409 area. Intermediate values are found in the Rocky Mountains and in the Western Cordillera.
410 This indicates that the reincorporation of Li into secondary phases is more important in the
411 lowlands and main tributaries than in the Cordillera and Rocky Mountain samples. In Figure
412 6, the dissolved Li/Na in the Shield rivers were normalized to the Prosperous Lake till
413 sample. If the till sample CAN96-31 (Yellowknife) is used as a reference for the parent
414 bedrock in the Slave Province, then f_{Li} values higher than 1 are found. Values of f_{Li} higher
415 than 1 would mean a preferential leaching of Li compared to Na. Although Prosperous Lake
416 till sample is our preferred bedrock estimate here, we nevertheless consider f_{Li} higher than 1
417 (and CAN96-31 as a source rock) as a possible scenario. Despite these uncertainties on the
418 bedrock in the Shield province, f_{Li} provides a relative indication of Li mobility during
419 weathering.
420 When the isotopic composition of dissolved lithium is plotted as a function of f_{Li}, a correlation
421 appears (Figure 6). This correlation can be explained by a binary mixing between waters
422 draining areas characterized by two markedly different weathering regimes.
423 The first end-member needed to account for the correlation between f_{Li} and δ^7Li of the
424 dissolved load corresponds to a weathering regime where Li is significantly precipitated in
425 the solids compared to Na, most probably incorporated into Li-rich secondary minerals
426 (clays). The lowlands and the transition zone areas best characterize this weathering regime
427 since they display the lowest f_{Li} values. Numerous studies have shown that Li isotopes are

428 fractionated during the formation of secondary minerals. The ~13‰ isotopic shift between the
429 composition of the dissolved load and the bedrock in the lowlands is, to a first order,
430 compatible with the estimated clay-solution isotopic fractionation at equilibrium (Taylor and
431 Urey 1938, Chan et al. 1992, Zhang et al. 1998, Pistiner and Henderson 2003, Vigier et al.
432 2008). The formation of secondary solids, being kinetically limited, requires a favorable
433 environment. Using boron isotopes, Lemarchand and Gaillardet (2006) have suggested that
434 most of the dissolved boron in rivers is derived from the shallow groundwater system (drift
435 aquifers). As shown by Lemay (2002), high lithium concentrations (3-15 µmol/L) are also
436 measured in these groundwaters. The correlation between boron and lithium concentrations
437 that links both rivers and groundwaters (Figure 7) strongly argues for a significant input of Li
438 to the lowland rivers from groundwaters. Because groundwaters have long residence times
439 relative to surface waters, chemical weathering reactions can proceed further than in the
440 Shield or Rocky Mountains areas where the residence time of water is not sufficiently long
441 (Lemarchand and Gaillardet 2006). We therefore suggest that the residence time of water in
442 groundwater counteracts the effect of low temperature and favors the formation of secondary
443 minerals that fractionate Li isotopes (Figure 6) at equilibrium.
444 The second endmember in Figure 6 corresponds to the Shield and Rocky Mountains areas,
445 and displays the highest δ^7Li and f_{Li} values. This situation may appear as a paradox because
446 f_{Li} indicates no or low Li incorporation in secondary products of weathering, while the isotopic
447 shift between Li in the bedrock and dissolved Li is at its maximum (from +16 to +22‰). The
448 Rocky Mountains and the Shield province are areas characterized by particularly low
449 chemical weathering rates (Millot et al. 2003), in contrast to the lowlands. These regions
450 have been deglaciated relatively recently and are characterized by abundant bare rocks and
451 poorly developed soils. The Rocky and Mackenzie Mountains areas have relatively high river
452 sediment yields with sediments mostly derived from glacial erosion (Millot et al. 2003) and
453 not from soils. The Shield area is characterized by important glacial till deposits. Several
454 hypotheses can be invoked to explain the enrichment of ^{7}Li in the waters of the Rocky
455 Mountains and of the Shield area. The most evident possibility is that the formation of some

456 secondary mineral fractionating Li isotopes. As indicated by the f_{Li} values close to 1, the
457 incorporation of Li into secondary phases should not be quantitatively important in these
458 regions but should however be visible in terms of isotope fractionation. A good candidate is
459 Mn and Fe-oxyhydroxide minerals. Adsorption of Li onto Fe and Mn oxyhydroxide surfaces
460 have been reported by Chan and Hein (2007) with preferential enrichment of ^{6}Li in the
461 deposit, thus consistent with the observed heavy isotope enrichment in the fluids. A recent
462 study reports the enrichment of the heavy isotope of Li in the dissolved load of glacial and
463 non-glacial rivers from Greenland and attributes it to the preferential uptake of ^{6}Li during
464 inner sphere sorption of Li^{+} on the Fe-oxyhydroxide surfaces (Wimpenny et al. 2010). The
465 same mechanism can be invoked here. The difference between the study of Wimpenny et al.
466 (2010) and our study is that the Shield rivers, that have ^{7}Li-enriched waters, are not sulfate-
467 rich and therefore that sulfide oxidation, a mechanism proposed by the authors to explain the
468 abundance of Fe-oxides in Greenland, is not applicable to the Shield rivers. The presence of
469 Fe-oxyhydroxides minerals in the Shield rivers could be tested by analysing Mn and Fe river
470 deposits often found in river bedloads, at the surface of blocks and boulders for example. In
471 addition, saturation state calculations (using PHREEQC modelling) indicate that the waters
472 are supersaturated with respect to goethite in this area.
473 A second possibility to explain the enrichment of ^{7}Li in the dissolved load of the Shield and
474 Mackenzie Mountain rivers could be a fractionation of Li isotopes during mineral dissolution.
475 Experimental work on basalt dissolution does not show evidence of Li isotope fractionation
476 during dissolution (Pistiner and Henderson 2003), but we can imagine a number of natural
477 processes potentially able to fractionate Li isotopes during mineral dissolution. The
478 preferential release of ^{7}Li could be possible either by the preferential dissolution of ^{7}Li-
479 enriched phases, or as a transient effect of the leaching process with formation of unstable
480 secondary phases such as Si-gel layers around minerals. So far, Li isotope heterogeneity at
481 the mineral scale has not been observed within a single bedrock, but we cannot exclude the
482 existence of low temperature minerals that would show ^{7}Li enrichments. What is interesting
483 here, is that the ^{7}Li enrichment in waters is observed in the geological context of glacial

484 erosion (still active in the Rockies and in the form of glacial deposits in the Shield area). The
485 abundance of fine glacial flour allows specific weathering reactions to occur, that have been
486 observed experimentally (in columns of grind granitic material, White et al. 1998) or in nature
487 (Anderson et al. 1989). In particular fast dissolving accessory phases like carbonates and
488 sulfides have been shown to contribute significantly to solute export in the early stages of
489 weathering.
490 Whatever the reason for Li isotope fractionation, our data do show that incipient weathering
491 of rocks can produce ^{7}Li enriched fluids. The similar enrichments found in Greenland
492 (Wimpenny et al. 2010) or in very recently deglaciated moraine in the granitic Swiss Alps
493 (Lemarchand et al. 2009) shows that Li isotopes are very sensitive to the early stages of
494 chemical weathering. Future studies will be necessary to investigate Li isotope fractionation
495 in incipient weathering conditions and the isotopic heterogeneity of bedrocks to precisely
496 determine the mechanisms that result in the preferential release of heavy Li isotopes in
497 solution.
498 According to the above discussion, all sampled rivers in the Mackenzie Basin have an
499 isotopic composition reflecting a mixture of water masses that have interacted with bedrock
500 minerals according to two contrasting weathering regimes. On one hand, oxyhydroxide
501 formation and/or leaching of comminuted bedrock produces ^{7}Li-enriched waters, similarly to
502 that occurring in glacial and non glacial rivers from Greenland. On the other hand, the more
503 optimum weathering conditions of the low-lying plain aquifers will produce waters with Li
504 isotopic compositions lower by about 20‰. As indicated by the previous studies of our group,
505 the weathering rates of silicates in these two contrasted environments differ by a factor of 3-
506 4, probably accelerated in the lowlands by the contribution of groundwaters (Lemarchand
507 and Gaillardet 2006) and the chelating effects of organic matter (Millot et al. 2003). The Li
508 isotopic data presented here show that the Li isotopic signature of waters is more influenced
509 by the precipitation of specific secondary phases than weathering rates. The relationship
510 between chemical weathering rates of silicates (calculated from the inversion of major
511 element concentrations and Sr isotopic ratios by Millot et al. 2003), and δ^{7}Li measured in the

512 dissolved loads is shown on Figure 8a. There is no clear relationship at the scale of the
513 Mackenzie River Basin between the Li isotopic composition and the specific flux of chemical
514 denudation, showing that secondary mineral formation is not necessarily related to
515 denudation fluxes. In particular, the high fluxes observed for the Western Cordillera and
516 visible in Figure 8 are due to the combined effects of runoff and the volcanic nature of
517 bedrocks (Gaillardet et al. 2003). The absence of a relationship between chemical
518 denudation rate and water lithium isotopic composition is in contrast with the relationship
519 observed on small monolithologic rivers in Iceland (Vigier et al. 2009).
520 Two trends of δ^7Li with total dissolved load derived from silicate weathering in mg/L are
521 observed (Figure 8b), corresponding to the two weathering regimes described above. The
522 first trend of increasing ^{7}Li-enrichment with dissolved solutes only contains samples from the
523 Shield and Rocky-Mackenzie Mountains from the first weathering regime described above.
524 By contrast, the waters most influenced by the second weathering regime show constant Li
525 isotopic composition with total dissolved load concentration derived from silicate weathering.
526 Figure 8b confirms the broad idea that Li isotopes are indicative of the regime weathering.
527 Regimes characterized by secondary clay formation have Li isotopic composition between 10
528 and 15‰ and show no relationship with silicate weathering rates, while weathering regimes
529 characterized by incipient weathering, or weathering of comminuted bedrocks, are
530 characterized by higher Li isotopic composition.
531

532 ## 6. CONCLUSIONS

533
534 The Li isotopic composition measured in the rivers of the Mackenzie Basin shows that ^{7}Li is
535 enriched in the dissolved load and that δ^7Li can vary by 20‰ within a large river basin. The
536 δ^7Li of the particulate load reflects that of the bedrock and ranges between -2 and +3‰. Our
537 study shows that dissolved Li in river waters is essentially derived from the weathering of
538 silicates and that Li isotopic ratios of the dissolved load depends on the weathering regime of
539 silicates.

If Na is considered as a soluble element not incorporated in secondary phases, river waters showing Li/Na ratios much lower than the bedrock ratio have the lowest isotopic compositions. Although the fractionation coefficients between solution and newly formed solids remain poorly known and need to be better constrained by experimental work, our isotopic data are consistent with the incorporation of Li into clay minerals at equilibrium. Groundwaters, in particular shallow aquifers in the low-lying plains of the basin, seem to play an important role in the acquisition of the dissolved Li isotope composition, probably because high residence times favor the formation of clay mineral. The most ^{7}Li-enriched waters are observed in the Rocky Mountains and in the Shield areas of the basin. In these areas, by analogy to previous work in Greenland (Wimpenny et al. 2010), we suggest that high δ^{7}Li values in rivers result from the fractionation associated with Li sorption onto Mn and Fe-oxyhydroxide surfaces. However, another mechanism could be that leaching is likely to be a non negligible process of water-rock interaction due to surficial or incipient weathering, being able to produce ^{7}Li-enriched waters. Experimental work will be necessary for better understanding the behaviour of Li isotopes in incipient weathering regimes.

To summarize, this large scale study shows that dissolved Li is essentially derived from silicate weathering but shows that silicate weathering does not have a unique isotopic signature. A very large variability of Li isotopic ratios exists within the Mackenzie Basin and is strongly spatialized. This is an important result if Li isotopes in the ocean are to be used as a proxy for the secular evolution of the Earth's surface. This study suggests that, rather than weathering fluxes, the weathering regime controls the Li isotopic signature of silicate weathering. Future work will have to address the role of the different parameters that define the weathering regime: time, climate, hydrological setting, residence time of water, biological parameters.

Acknowledgements:

This work was supported by the French program funded by the INSU-CNRS (PNSE contribution 322). We would like to express special thanks to B. Dupré for measurements of trace elements in Toulouse University. We also would like to acknowledge B. Dupré, C. Gariépy and D. Lemarchand for their help in collecting river samples. We thank E. Lemarchand and E.T. Tipper for fruitful discussions. RM would like to thank Ph. Négrel and T.D. Bullen for comments in an earlier version of the manuscript and the Research Division of BRGM is also acknowledged for funding. We thank R. James, P. Pogge van Strandmann and B. Reynolds for providing critical comments that improved this manuscript. D. Vance is also thanked for editorial handling and constructive comments. Finally, we also would like to thank P. Burnard and R.H. Hilton for comments and English corrections. This is IPGP contribution n° 2581 and BRGM contribution n° 6327.

580 **References**

581

582 Anderson M.A., Bertsch P.M., and Miller W.P. (1989) Exchange and apparent fixation of
583 Lithium in selected soils and clay minerals. Soil Sci., 148, 46-52.

584 Anghel I., Turin H.J., and Reimus P.W. (2002) Lithium sorption to Yucca mountain tuffs.
585 Appl. Geochem., 17, 819-824.

586 Calmels D., Gaillardet J. Brenot A., France-Lanord C. (2007) Sustained sulfide oxidation by
587 physical erosion processes in the Mackenzie River basin: Climatic perspectives. Geology,
588 35: 1003-1006.

589 Carignan J., Cardinal D., Eisenhauer A., Galy A., Rehkämper M., Wombacher F., Vigier N.
590 (2004) A reflection on Mg, Ca, Cd, Li and Si isotopic measurements and related reference
591 materials. Geostandards and Geoanalytical Research, 28: 139-148.

592 Carignan J., Vigier N., Millot R. (2007) Three secondary reference materials for Li isotopic
593 measurements: ^{7}Li-N, ^{6}Li-N and LiCl-N. Geostandards and Geoanalytical Research, 31: 7-
594 12.

595 Chan L.H., Edmond J.M. Thompson G., Gillis K. (1992) Lithium isotopic composition of
596 submarine basalts: implications for the lithium cycle to the ocean, Earth Planet. Sci. Lett.,
597 108: 151-160.

598 Chan L.H., Hein J.R. (2007) Lithium contents and isotopic compositions of ferromanganese
599 deposits from the global ocean. Deep-sea research part II – topical studies in
600 Oceanography, 54: 1147-1162.

601 Flesch G.D., Anderson A.R., Svec H.J. (1973) A secondary isotopic standard for ^{6}Li/^{7}Li
602 determinations. International Journal of Mass Spectrometry and Ion Physics, 12: 265-272.

603 Gaillardet J., Dupré B., Louvat P., Allègre C.J. (1999) Global silicate weathering and CO_2
604 consumption rates deduced from the chemistry of large rivers. Chemical Geology, 159: 3-
605 30.

606 Gaillardet J., Millot R., Dupré B. (2003) Chemical denudation rates of the western Canadian
607 orogenic belt: the Stikine terrane. Chemical Geology, 201: 257-279.

608 Georg R.B., Reynolds B.C., West A.J., Burton K.W., Halliday A.N. (2007) Silicon isotope
609 variations accompanying basalt weathering in Iceland. Earth and Planetary Science
610 Letters, 261: 476-490.
611 Hall J.M., Chan L.H. (2004) Li/Ca in multiple species of benthic and planktonic foraminifera:
612 thermocline, latitudinal, and glacial-interglacial variation. Geochimica et Cosmochimica
613 Acta, 68: 529-545.
614 Hall J.M. , Chan L.H., McDonough W.F., Turekian K.K. (2005) Determination of the lithium
615 isotopic composition of planktic foraminifera and its application as a paleo-seawater proxy.
616 Marine Geology, 217: 255-265.
617 Hathorne E.C., James R.H. (2006) Temporal record of lithium in seawater: A tracer for
618 silicate weathering? Earth and Planetary Science Letters, 246: 393-406.
619 Hathorne E.C., James R.H. Lampitt R.S. (2009) Environmental versus biomineralization
620 controls on the intratest variation in the trace element composition of the planktonic
621 foraminifera G. inflata and G. scitula. Paleoceanography, 24: PA4204.
622 Holland H.D. (1978) The chemistry of oceans and atmosphere, Wiley and Sons, New York.
623 Huh Y., Chan L.C., Zhang L., Edmond J.M. (1998) Lithium and its isotopes in major world
624 rivers: implications for weathering and the oceanic budget. Geochimica et Cosmochimica
625 Acta, 62: 2039-2051.
626 Huh Y., Chan L.C., Edmond J.M. (2001) Lithium isotopes as a probe of weathering
627 processes: Orinoco River. Earth and Planetary Science Letters, 194: 189-199.
628 Huh Y., Chan L.C., Chadwick O.A. (2004) Behavior of lithium and its isotopes during
629 weathering of Hawaiian basalt. Geochemistry, Geophysics, Geosystems, 5: 1-22.
630 James R.H., Palmer M.R. (2000) The lithium isotope composition of international rock
631 standards. Chemical Geology, 166: 319-326.
632 Jeffcoate A.B., Elliott T., Thomas A., Bouman C. (2004) Precise, small sample size
633 determinations of lithium isotopic compositions of Geological Reference Materials and
634 modern seawater by MC-ICP-MS. Geostandards and Geoanalytical Research, 28: 161-
635 172.

636 Kisakürek B., Widdowson M., James R.H. (2004) Behaviour of Li isotopes during continental
637 weathering: the Bidar laterite profile, India. Chemical Geology, 212: 27-44.
638 Kisakürek B., James R.H., Harris N.B.W. (2005) Li and δ^7Li in Himalayan rivers: Proxies for
639 silicate weathering? Earth and Planetary Science Letters, 237: 387-401.
640 Lear C.H., Rosenthal Y. (2006) Benthic foraminiferal Li/Ca: insights into Cenozoic seawater
641 carbonate saturation state. Geology, 34: 985-988.
642 Lemarchand D., Gaillardet J. (2006) Transient features of the erosion of shales in the
643 Mackenzie basin (Canada), evidences from boron isotopes. Earth and Planetary Science
644 Letters, 245: 174-18.
645 Lemarchand E., Tipper E.T., Hindshaw R., Wiederhold J.G., Reynolds B.C., Bourdon B.,
646 Kretzchmar R. (2009) Li isotope fractionation in surface waters of an alpine granitic
647 catchment. Goldschmidt Conference Abstract A742.
648 Lemay T.G. (2002) Geochemical and isotope data for formation water from selected wells,
649 cretaceous to quaternary succession, Athabasca oil sand (in situ) area, Alberta, EUB/AGS
650 Geo-Note 2002-02: 1-30.
651 Millot R., Gaillardet J., Dupré B., Allègre C.J. (2002) The global control of silicate weathering
652 rates and the coupling with physical erosion: new insights from the Canadian Shield. Earth
653 and Planetary Science Letters, 196: 83-98.
654 Millot R., Gaillardet J., Dupré B., Allègre C.J. (2003) Northern latitude chemical weathering
655 rates: clues from the Mackenzie River Basin, Canada. Geochimica et Cosmochimica Acta,
656 67: 1305-1329.
657 Millot R., Guerrot C., Vigier N. (2004) Accurate and high-precision measurement of lithium
658 isotopes in two reference materials by MC-ICP-MS. Geostandards and Geoanalytical
659 Research, 28: 153-159.
660 Négrel Ph., Allègre C.J., Dupré B., Lewin E. (1993) Erosion sources determined by inversion
661 of major and trace element ratios and strontium isotopic ratios in river water: the Congo
662 Basin case. Earth and Planetary Science Letters, 120: 59-76.

663 Pistiner J.S., Henderson G.M. (2003) Lithium isotope fractionation during continental
664 weathering processes. Earth and Planetary Science Letters, 214: 327-339.
665 Pogge von Strandmann P.A.E., Burton K.W., James R.H., van Calsteren P., Gislason S.R.,
666 Mokadem F. (2006) Riverine behaviour of uranium and lithium isotopes in an actively
667 glaciated basaltic terrain. Earth and Planetary Science Letters, 251: 134-147.
668 Reeder S.W., Hitchon B., Levinson A.A. (1972) Hydrogeochemistry of the surface waters of
669 the Mackenzie River drainage basin, Canada-I. Factors controlling inorganic composition.
670 Geochimica et Cosmochimica Acta, 36: 825-865.
671 Rudnick R.L., Tomascak P.B., Njo H.B., Robert Gardner L. (2004) Extreme lithium isotopic
672 fractionation during continental weathering revealed in saprolites from South Carolina.
673 Chemical Geology, 212: 45-57.
674 Taylor S.R., Urey H.C. (1938) Fractionation of the lithium and potassium isotopes by
675 chemical exchange with zeolites, J. Chem. Phys. 6: 429-438.
676 Taylor S.R., MacLennan S.M. (1985) The continental crust: its composition and evolution,
677 Blackwell Scientific Publications, 312 p.
678 Teng F.Z., McDonough W.F., Rudnick R.L., Dalpé C., Tomascak P.B., Chappell B.W., Gao
679 S. (2004) Lithium isotopic composition and concentration of the upper continental crust.
680 Geochimica et Cosmochimica Acta, 68: 4167-4178.
681 Teng F.Z., McDonough W.F., Rudnick R.L., Walker R.J. (2006) Diffusion-driven extreme
682 lithium isotopic fractionation in country rocks of the Tin Mountain pegmatite. Earth and
683 Planetary Science Letters, 243: 701-710.
684 Teng F.Z., Rudnick R.L., McDonough W.F., Gao S., Tomascak P.B., Liu Y. (2008) Lithium
685 isotopic composition and concentration of the deep continental crust. Chemical Geology,
686 255: 47-59.
687 Teng F.Z., Rudnick R.L., McDonough W.F., Wu F.Y. (2009) Lithium isotopic systematics of
688 A-type granites and their mafic enclaves: Further constraints on the Li isotopic
689 composition of the continental crust. Chemical Geology, 262: 370-379.

690 Tomascak P.B. (2004) Developments in the understanding and application of lithium
691 isotopes in the Earth and Planetary Sciences. Reviews in Mineralogy & Geochemistry, 55:
692 153-195.

693 Vigier N., Bourdon B., Turner S., Allègre C.J. (2001) Erosion timescales derived from U-decay
694 series measurements in rivers, Earth and Planetary Science Letters, 193: 549-563.

695 Vigier N., Rollion-Bard C., Spezzaferri S. and Brunet F. (2007) In-situ measurements of Li
696 isotopes in foraminifera. Geochemistry, Geophysics, Geosystems Q01003.

697 Vigier N., Decarreau A., Millot R., Carignan J., Petit S., France-Lanord C. (2008) Quantifying
698 Li isotope fractionation during smectite formation and implications for the Li cycle,
699 Geochimica et Cosmochimica Acta, 72: 780-792.

700 Vigier N., Gislason S.R., Burton K.W., Millot R., Mokadem F. (2009) The relationship
701 between riverine lithium isotope composition and silicate weathering rates in Iceland.
702 Earth and Planetary Science Letters, 287: 434-441.

703 White A.F., Blum A.E., Schulz M.S., Vivit D.V., Larsen M., Murphy S.F. (1998) Chemical
704 weathering in a tropical watershed, Luquillo Mountains, Puerto Rico: I. Long-term versus
705 short-term chemical fluxes. Geochimica et Cosmochimica Acta, 62: 209-226.

706 Wimpenny J., James R.H., Burton K.W., Gannoun A., Mokadem F., Gíslason S.R. (2010)
707 Glacial effects on weathering processes: New insights from the elemental and lithium
708 isotopic composition of West Greenland rivers. Earth and Planetary Science Letters, 290:
709 427-437.

710 Zhang L., Chan L.H., Gieskes J.M. (1998) Lithium isotope geochemistry of pore waters from
711 Ocean Drilling Program Sites 918 and 919, Irminger Basin, Geochim. Cosmochim. Acta
712 62: 2437-2450.

713 **Figure captions**

714

715 **Figure 1**

716 Map showing the sample locations within the Mackenzie River Basin and adjacent basins
717 (Yukon, Stikine, Nass, Skeena and Fraser Basin).

718

719 **Figure 2**

720 Inverse correlation of Li isotopic composition and Li concentration in the dissolved load. In
721 this diagram, the geomorphorphic provinces of the Mackenzie river basin are well
722 distinguished.

723

724 **Figure 3**

725 Histogram for Li contribution coming from silicate weathering (%) in Mackenzie river water
726 samples.

727

728 **Figure 4**

729 Histogram of Li isotopic composition in the dissolved and suspended loads of the Mackenzie
730 rivers. Bedrock values from this study (4 values) and from a compilation of literature data on
731 shale, granite and loess (Teng et al. 2004) are added for comparison. This figure clearly
732 shows the ^{7}Li enrichment of the dissolved phase compared to bedrocks, while suspended
733 sediments and bedrocks are essentially similar.

734

735 **Figure 5**

736 Lithium isotopic composition in the suspended sediments of the Mackenzie rivers (main
737 tributaries, Rocky and Mackenzie Mountains, Interior Platform and transition mountain/plain)
738 and glacial till sample (Canadian Shield) as a function of Na/Al ratio. This ratio can be seen
739 as a proxy for Na loss compared to Al, and is therefore a weathering intensity proxy. Na loss
740 can be attributed either to present day weathering processes or to previous episodes of

741 weathering that would have occurred during the geological history of the sedimentary
742 bedrocks.
743
744 **Figure 6**
745 Lithium isotopic composition in the dissolved load as a function of f_{Li}. f_{Li} represents the
746 relative mobility of Li with respect to Na, an element not generally known to be
747 reincorporated into secondary phases. This parameter is defined as the ratio of Li/Na in the
748 dissolved load to that in the suspended sediments or, in the case of the Shield province, to
749 the Prosperous Lake moraine. Na* denotes here that the Na concentrations are corrected for
750 atmospheric input and, for a couple of rivers, are corrected for evaporite dissolution
751 according to the results of Millot et al. (2003). Ratios in suspended sediments are considered
752 to represent bedrock ratios. For the Shield rivers, if the glacial till (sample CAN96-31) is used
753 for normalizing the Li/Na data from the shield rivers then f_{Li} values higher that 1 would be
754 obtained for these rivers (not shown on the figure), but lithium isotopic composition and f_{Li} are
755 still correlated.
756
757 **Figure 7**
758 Relationship between boron and lithium concentrations in the dissolved load of the rivers
759 sampled in this study. Data from drift aquifers reported by Lemay et al. (2002) have been
760 added to show that the contribution from a groundwater input is likely. Boron data are from
761 Lemarchand and Gaillardet (2006). Boron isotopic data strongly suggest that boron isotopic
762 composition was acquired during reactive transport of boron in shallow groundwaters of
763 relatively high water residence time, and that, boron is therefore a good tracer of the
764 groundwater contribution.
765
766 **Figure 8**
767 Li isotopic composition as a function of Silicate Weathering Rate (Figure 8a) and Silicate
768 Weathering Load (Figure 8b) for the river samples. Silicate weathering rates were calculated

769 in Millot et al. (2003) based on the inversion of major element concentration and Sr isotope
770 data in the dissolved load, and by Gaillardet et al. (2003) for the Stikine province. In Figure
771 8b, the observed feature is consistent with the idea developed here that the Li isotopic
772 composition of water in the Mackenzie basin rivers reflects mixing between waters modified
773 by weak (incipient or surficial) weathering (weathering regime #1) and waters dominated by
774 more intense water-rock interactions with the formation of secondary phases in the lowlands
775 of the Mackenzie River Basin (weathering regime #2).

776 **Table captions**

777

778 **Table 1**

779 Lithium isotopic composition δ^7Li (‰) and concentrations (µmol/L) for rivers waters of the
780 Mackenzie Basin and the W. Cordillera. Analytical precision for each δ^7Li measurement is
781 reported in this table and range from 0.1 to 0.3‰ ($2\sigma_m$). As mentioned in the analytical
782 section, the total reproducibility is ± 0.5‰ (2σ) and has been determined by long-term
783 repeated measurements of a seawater sample (Millot et al. 2004). Surface area (km^2), river
784 discharge (km^2/year), runoff (mm/year) and Silicate Weathering Rates (tons/km^2/yr and mg/L)
785 have also been added in this table (from Millot et al. 2003).

786

787 **Table 2**

788 Lithium isotopic composition δ^7Li (‰) and concentrations (µg/g) in suspended sediments for
789 rivers from the Mackenzie Basin and adjacent basins draining the Canadian orogenic belt
790 (W. Cordillera). Na and Al concentrations are also given in µg/g.

791

792 **Table 3**

793 δ^7Li (‰) and Li concentrations (µg/g) in sand samples from the Mackenzie River at the river
794 mouth (CAN96-6), as well as in carbonate, blackshales, and two glacial tills sampled on the
795 Canadian Shield.

796

797

798 **Figure 1**

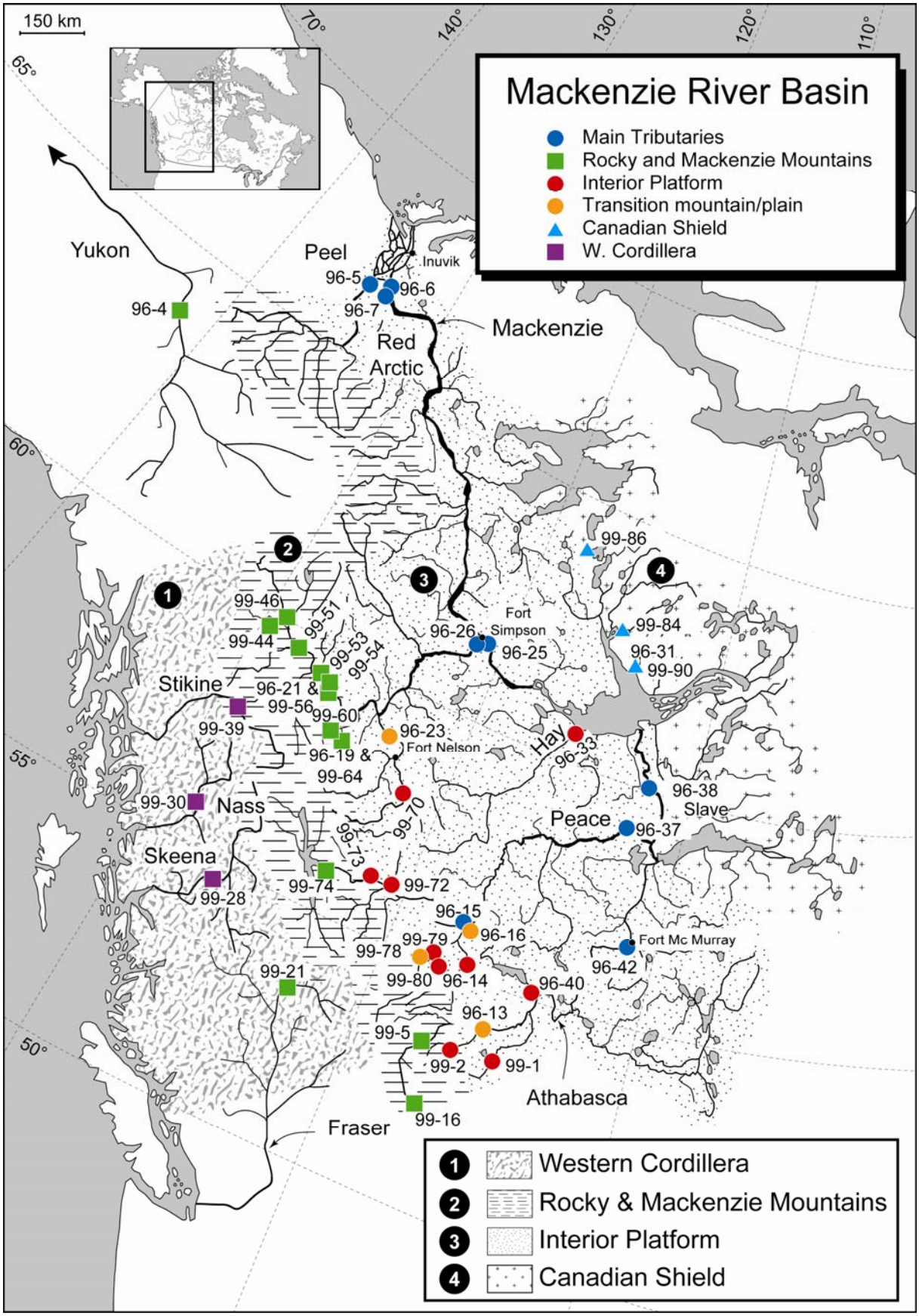

799

Figure 2

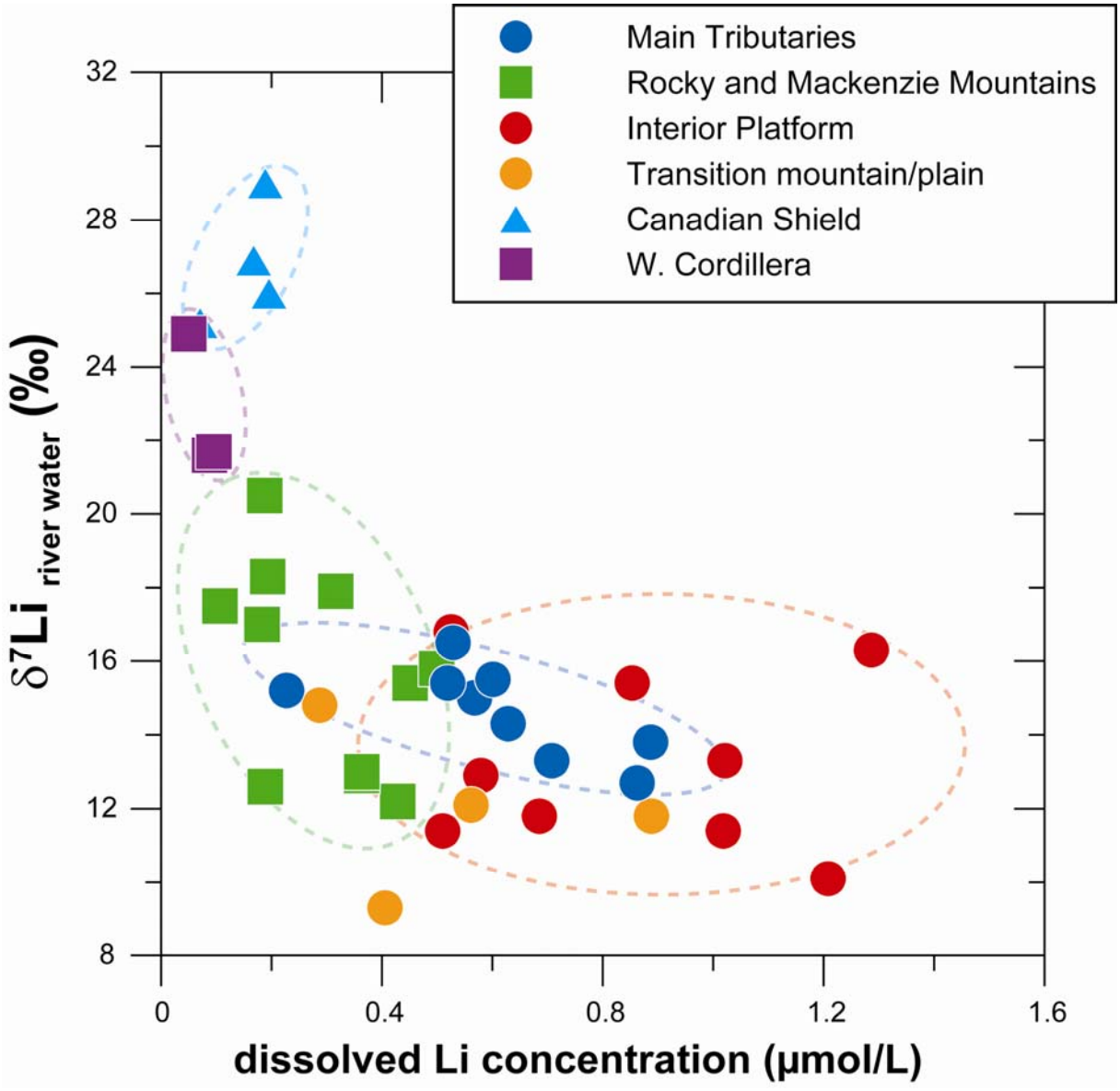
Main Tributaries
Rocky and Mackenzie Mountains
Interior Platform
Transition mountain/plain
Canadian Shield
W. Cordillera
32
28
24
20
16
12
8
0
0.4
0.8
1.2
1.6
δ7Li river water (‰)
dissolved Li concentration (µmol/L)

Figure 3

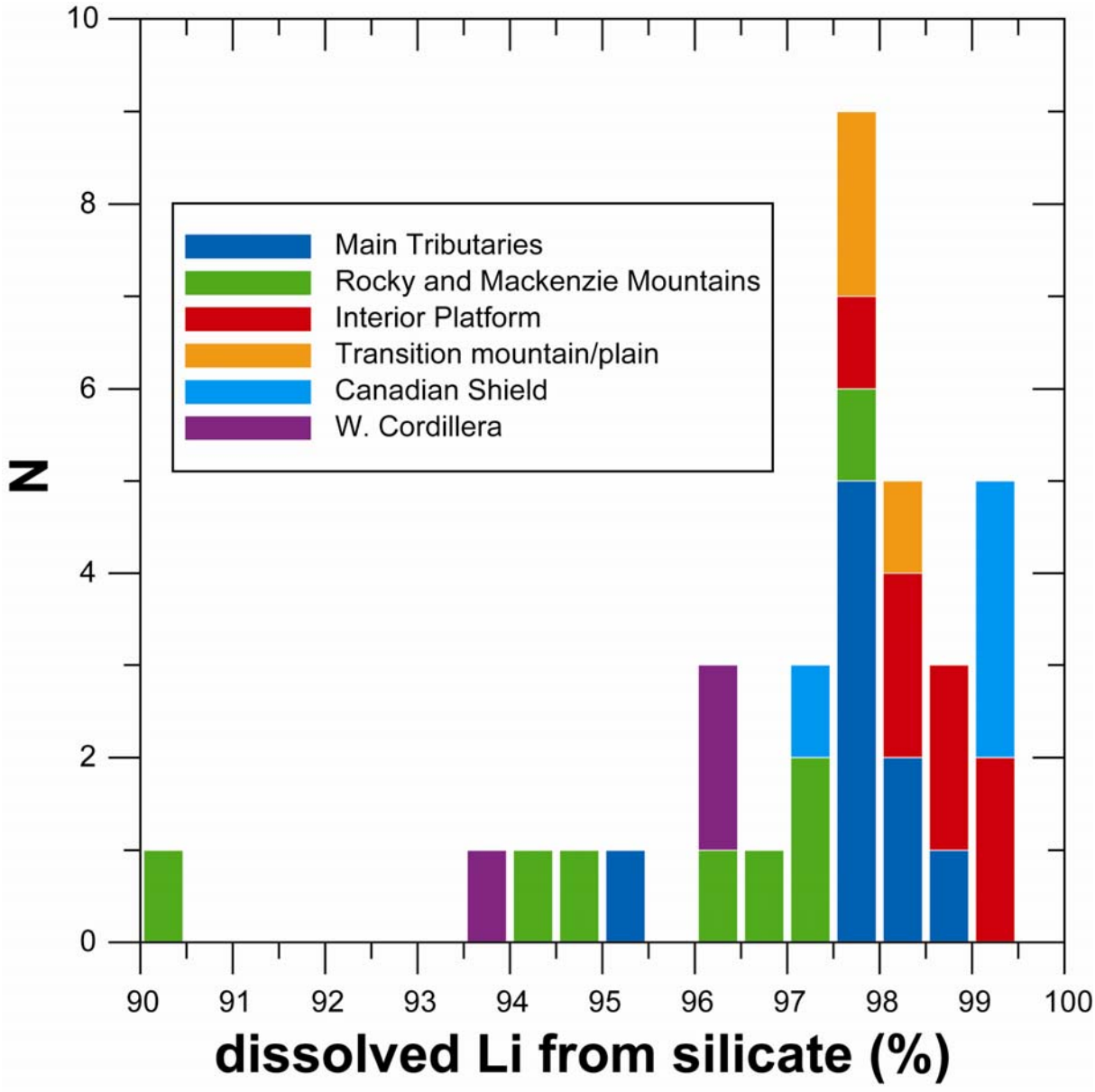
Main Tributaries
Rocky and Mackenzie Mountains
Interior Platform
Transition mountain/plain
Canadian Shield
W. Cordillera
N
dissolved Li from silicate (%)
0
2
4
6
8
10
90
91
92
93
94
95
96
97
98
99
100

814 **Figure 4**

815

816

817

818

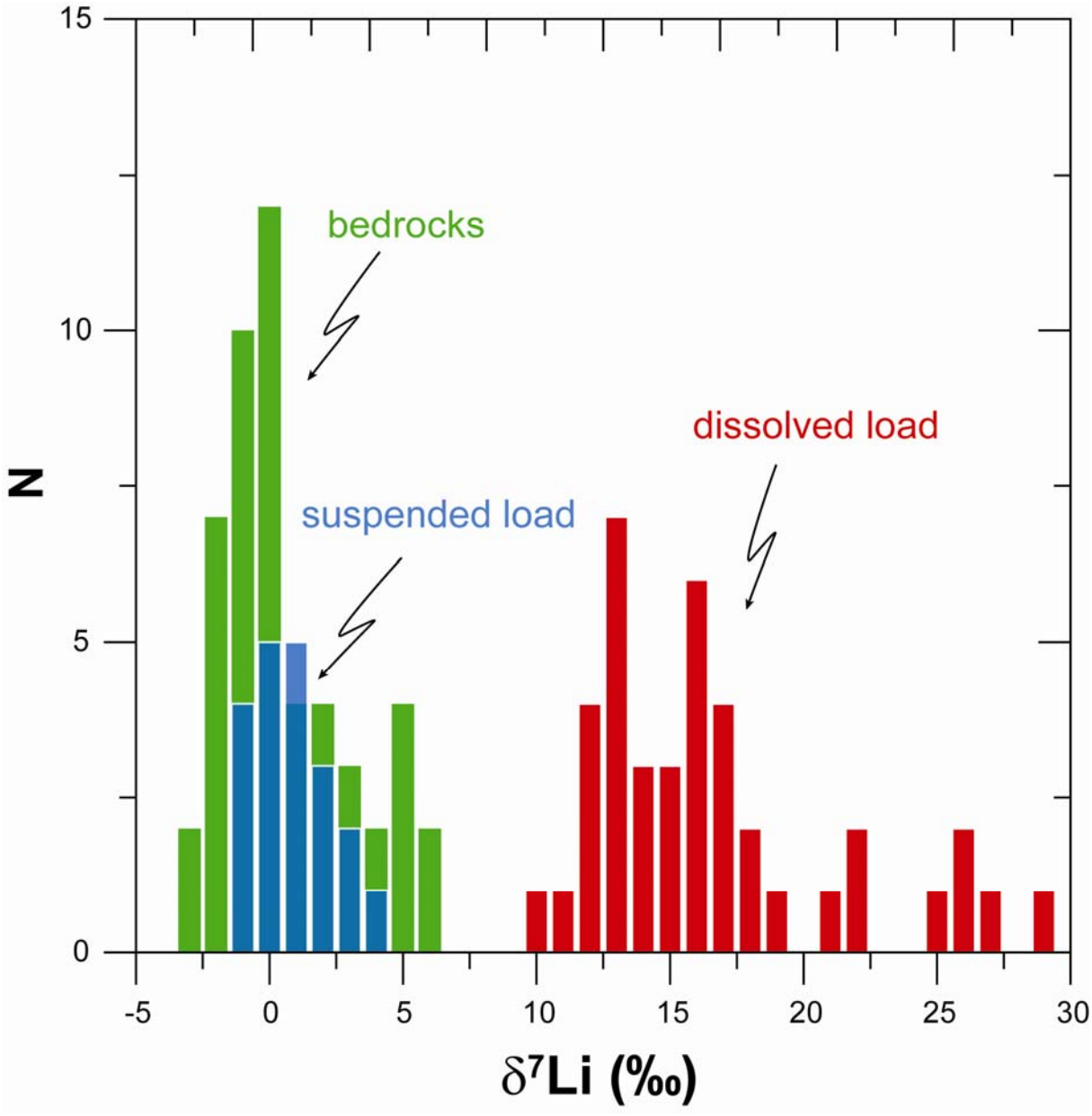

819

Figure 5

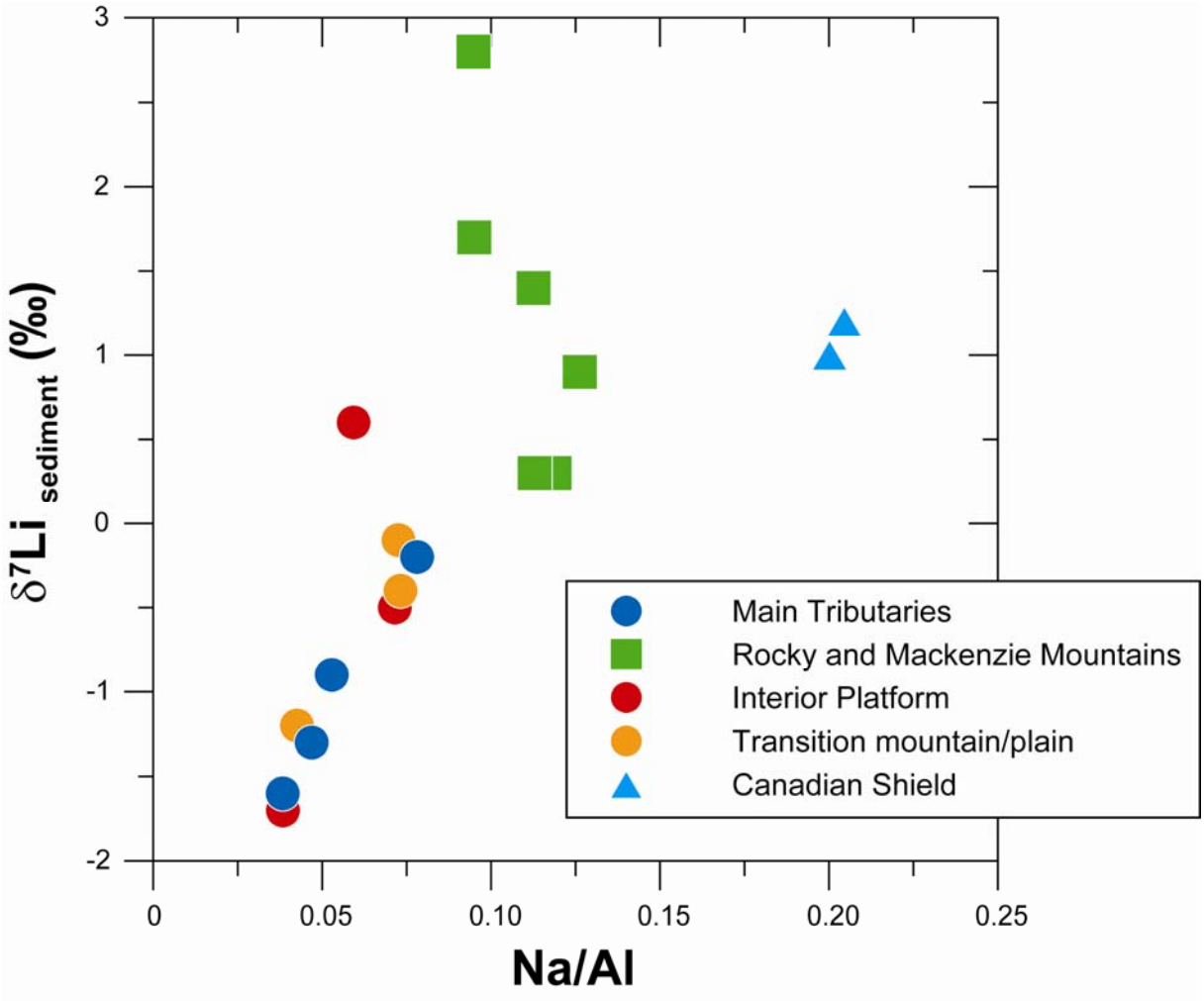
3
2
1
0
-1
-2
0
0.05
0.10
0.15
0.20
0.25
Na/Al
δ7Li sediment (‰)
Main Tributaries
Rocky and Mackenzie Mountains
Interior Platform
Transition mountain/plain
Canadian Shield

Figure 6

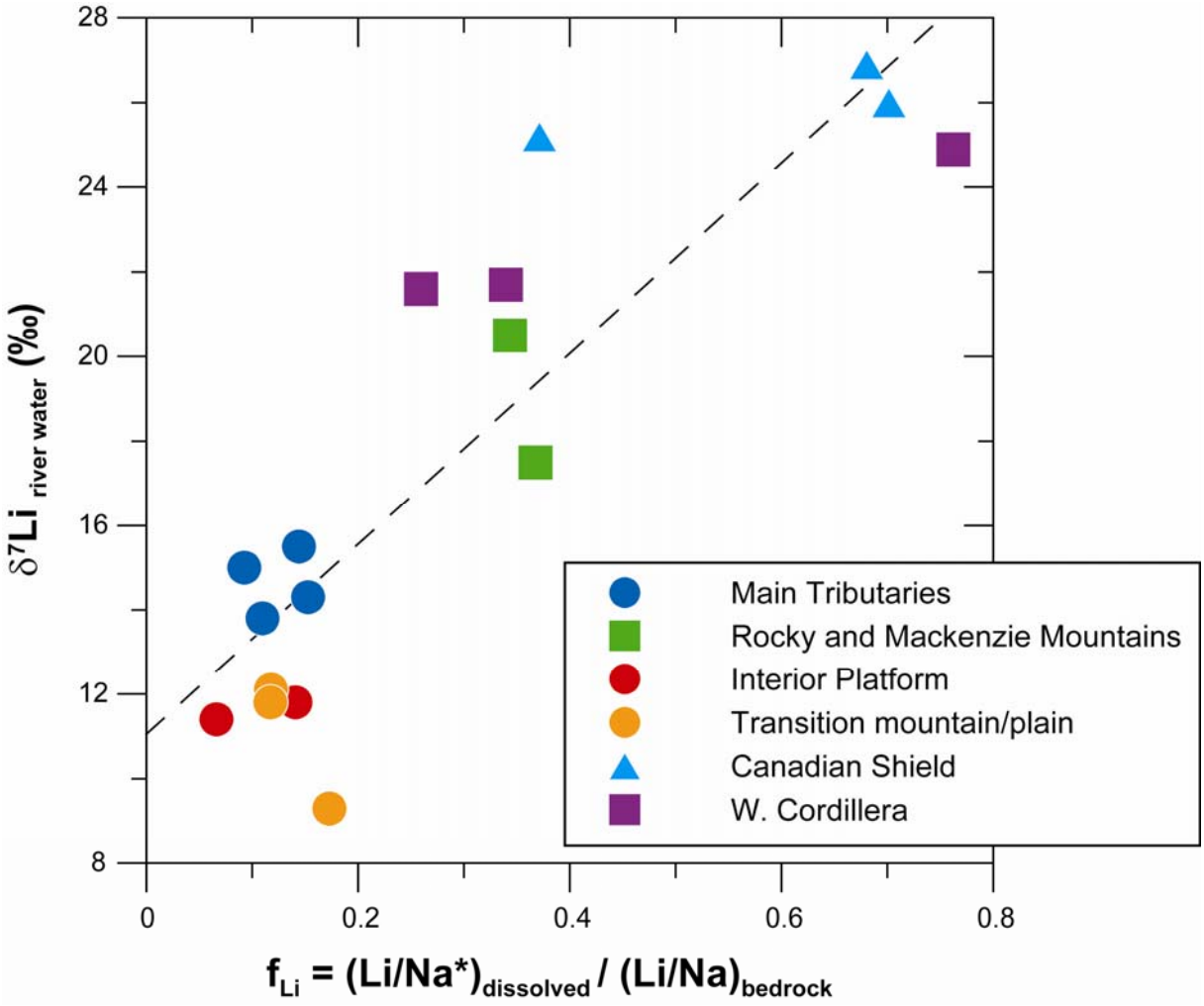
28
24
20
16
12
8
0
0.2
0.4
0.6
0.8
δ7Li river water (‰)
fLi = (Li/Na*)dissolved / (Li/Na)bedrock
Main Tributaries
Rocky and Mackenzie Mountains
Interior Platform
Transition mountain/plain
Canadian Shield
W. Cordillera

Figure 7

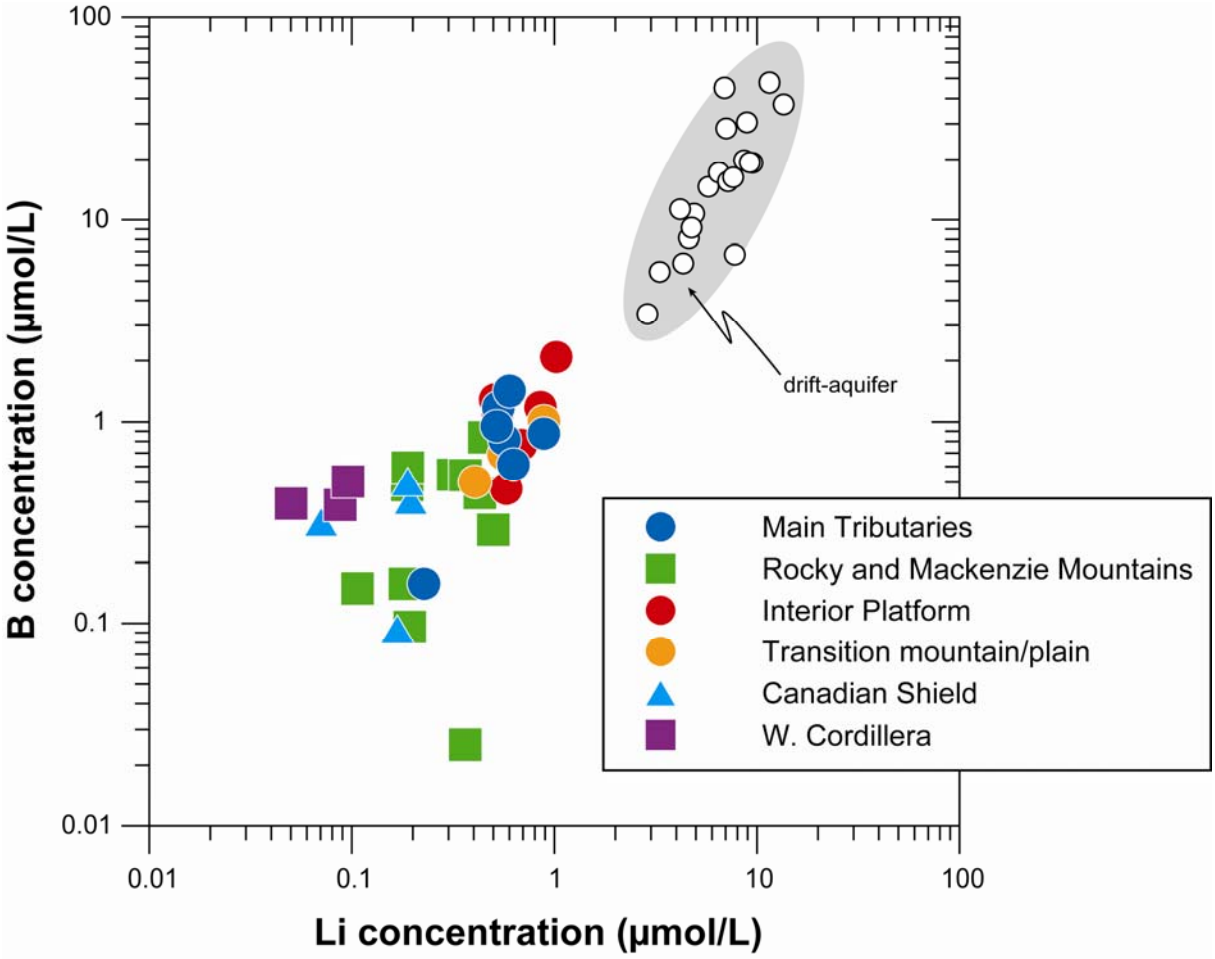
100
10
1
0.1
0.01
0.01
0.1
1
10
100
B concentration (µmol/L)
Li concentration (µmol/L)
drift-aquifer
Main Tributaries
Rocky and Mackenzie Mountains
Interior Platform
Transition mountain/plain
Canadian Shield
W. Cordillera

838 **Figure 8**

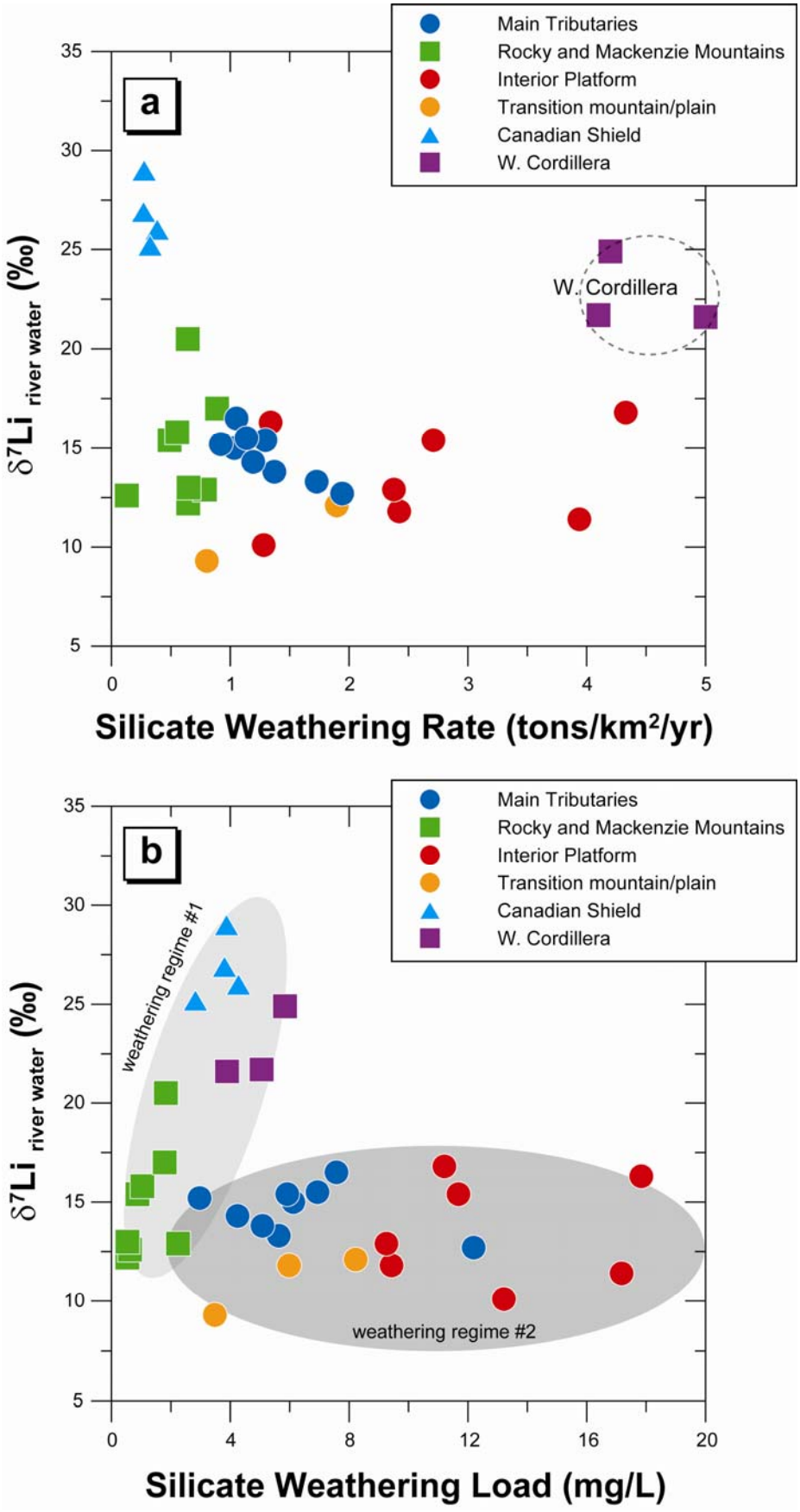

839

840 **Table 1**

841

Tributaries	sample number	River name	δ^7Li ‰	$2\sigma_m$	Li µmol/L	Area km^2	Discharge km^3/year	Runoff mm/year	Silicate Weathering Rate tons/km^2/year	mg/L
Main tributaries	CAN96-5	Peel (FortMcPherson)	+ 13.3	0.1	0.71	70600	21.65	307	1.73	5.63
	CAN96-6	Mackenzie (Tsiigehtchic)	+ 15.0	0.2	0.57	1680000	283.70	169	1.03	6.12
	CAN96-7	Red Arctic (Tsiigehtchic)	+ 13.8	0.1	0.89	18600	5.02	270	1.37	5.08
	CAN96-15	Peace (PeaceRiver)	+ 15.2	0.2	0.23	186000	57.75	310	0.92	2.96
	CAN96-25	Mackenzie (FortSimpson)	+ 16.5	0.3	0.53	1270000	137.90	139	1.05	7.57
	CAN96-26	Liard (FortSimpson)	+ 14.3	0.1	0.63	275000	77.32	281	1.19	4.24
	CAN96-37	Peace (PeacePoint)	+ 15.4	0.1	0.52	305500	67.01	219	1.30	5.92
	CAN96-38	Slave (FortSmith)	+ 15.5	0.2	0.60	616400	100.98	164	1.14	6.94
	CAN96-42	Athabasca (FortMcMurray)	+ 12.7	0.2	0.86	131000	20.86	159	1.94	12.19
Rocky and Mackenzie Mountains	CAN96-4	Yukon (Dawson)	+ 17.9	0.2	0.32	-	-	-	-	-
	CAN96-19	Racing	+ 12.2	0.1	0.43	1900	2.30	1209	0.65	0.53
	CAN99-5	Athabasca (Hinton)	+ 15.4	0.2	0.45	9780	5.46	558	0.49	0.88
	CAN96-21	Liard (LiardRiver)	+ 12.9	0.1	0.36	33400	11.71	351	0.79	2.24
	CAN99-21	Fraser	+ 17.5	0.1	0.11	-	-	-	-	-
	CAN99-46	Liard (UpperLiard)	+ 20.5	0.1	0.19	33400	11.71	351	0.64	1.83
	CAN99-54	Smith	+ 12.6	0.1	0.19	3740	0.77	207	0.13	0.62
	CAN99-56	Liard (LiardRiver)	+ 18.3	0.2	0.19	-	-	-	-	-
	CAN99-60	Toad	+ 15.8	0.1	0.50	2570	1.37	532	0.55	1.04
	CAN99-64	Racing	+ 13.0	0.1	0.36	1900	2.30	1209	0.65	0.54
	CAN99-74	Peace (Hudson'sHope)	+ 17.0	0.2	0.18	69900	34.71	497	0.89	1.79
Interior Platform	CAN96-14	Little Smoky	+ 11.8	0.2	0.69	3010	0.77	257	2.42	9.43
	CAN96-33	Hay (mouth)	+ 16.3	0.1	1.29	47900	3.60	75	1.34	17.84
	CAN96-40	Lesser Slave	+ 10.1	0.1	1.21	13600	1.32	97	1.28	13.21
	CAN99-1	Pembina (Evansburg)	+ 16.8	0.1	0.53	2900	1.12	386	4.33	11.21
	CAN99-2	Mc Leod	+ 15.4	0.1	0.85	9100	2.11	232	2.71	11.68
	CAN99-71	Doig	+ 13.3	0.1	1.02	-	-	-	-	-
	CAN99-72	Beatton	+ 11.4	0.1	0.51	-	-	-	-	-
	CAN99-79	Simonette	+ 11.4	0.1	1.02	5050	1.16	229	3.94	17.17
	CAN99-80	Little Smoky	+ 12.9	0.1	0.58	3010	0.77	257	2.38	9.26
Transition mountain/plain	CAN96-13	Athabasca	+ 14.8	0.2	0.29	-	-	-	-	-
	CAN96-16/1	Smoky	+ 12.1	0.1	0.56	51300	11.83	231	1.90	8.22
	CAN96-23	Fort Nelson	+ 11.8	0.1	0.89	-	-	-	-	5.98
	CAN99-78	Smoky	+ 9.3	0.1	0.41	51300	11.83	231	0.80	3.48
Canadian Shield	CAN96-31	Yellowknife	+ 26.9	0.1	0.17	16300	1.16	71	0.27	3.80
	CAN99-84	Wecho	+ 26.0	0.2	0.20	3400	0.31	90	0.39	4.28
	CAN99-86	Wopmay	+ 25.2	0.1	0.07	-	-	-	0.33	2.83
	CAN99-90	Yellowknife	+ 29.0	0.1	0.19	16300	1.16	71	0.28	3.87
W. Cordillera	CAN99-28	Skeena	+ 24.9	0.2	0.05	42200	30.36	719	4.20	5.84
	CAN99-30	Nass	+ 21.6	0.1	0.09	19200	24.68	1285	5.00	3.89
	CAN99-39	Stikine	+ 21.7	0.1	0.10	29300	23.83	811	4.10	5.06

842

843

844

845 **Table 2**

846

847

848

849

850

Tributaries	sample number	River name	δ^7Li	$2\sigma_m$	Li µg/g	Na µg/g	Al µg/g
Main tributaries	CAN96-6	Mackenzie (Tsiigehtchic)	- 0.9	0.2	57.8	3710	70200
	CAN96-7	Red Arctic (Tsiigehtchic)	- 1.6	0.1	56.8	2819	73535
	CAN96-26	Liard (FortSimpson)	- 1.3	0.2	46.1	3339	71206
	CAN96-38	Slave (FortSmith)	- 0.2	0.1	41.2	5268	67447
Rocky and Mackenzie Mountains	CAN99-5	Athabasca (Hinton)	+ 2.6	0.2	28.9	-	-
	CAN99-16	Athabasca (Falls)	+ 3.2	0.1	19.4	-	-
	CAN99-21	Fraser	+ 1.4	0.1	48.3	10387	92276
	CAN99-44	French	+ 1.7	0.2	17.9	4377	46059
	CAN99-46	Liard (UpperLiard)	+ 0.9	0.2	35.1	8235	65224
	CAN99-51	Hyland	+ 0.3	0.1	44.3	8458	71206
	CAN99-53	Coal	+ 0.3	0.1	46.2	7939	70306
	CAN99-57	Trout	+ 2.8	0.2	17.8	3042	32082
Interior Platform	CAN96-14	Little Smoky	- 0.5	0.1	37.8	5713	79888
	CAN99-72	Beatton	- 1.7	0.2	51.4	2968	77294
	CAN99-73	Halfway	+ 0.6	0.1	30.5	2968	50029
Transition mountain/plain	CAN96-16	Smoky	- 0.4	0.1	38.9	5565	76024
	CAN99-78	Smoky	- 0.1	0.1	35.3	4674	64376
	CAN96-23	Fort Nelson	- 1.2	0.2	56.1	3190	74965
W. Cordillera	CAN99-30	Nass	+ 1.0	0.2	37.6	14690	73376
	CAN99-39	Stikine	+ 1.2	0.1	24.5	15358	75071

851

852

Table 3

Tributaries	Sample type	sample number	sample name/location	δ^7Li	$2\sigma_m$	Li µg/g
Main tributaries	Sand	CAN96-6	Mackenzie @Tsiigehtchic	- 0.5	0.1	47.4
Rocky and Mackenzie Mountains	Black Shale	CAN99-5	Athabasca @Hinton	- 1.0	0.2	29.1
	Carbonate	CAN99-65	Mc Donald	+ 7.2	0.1	1.5
Transition mountain/plain	Black Shale	CAN99-70	Sikanni Chief	- 1.1	0.1	64.4
Canadian Shield	Glacial Till	CAN96-31	Yellowknife	+ 4.8	0.2	16.2
	Glacial Till		Prosperous Lake	+ 5.2	0.2	54.6